Progress In Electromagnetics Research M, Vol. 20, 127–141, 2011

INVERSE SOURCE PROBLEM: A COMPARISON BETWEEN THE CASES OF ELECTRIC AND MAGNETIC SOURCES

R. Solimene[1], C. Mola[1], R. Pierri[1], and F. Soldovieri[2, *]

[1]Dipartimento di Ingegneria dell'Informazione, Seconda Università di Napoli, Via Roma 29, Aversa 81031, Italy

[2]Istituto per il Rilevamento Elettromagnetico dell'Ambiente, CNR, Via Diocleziano 328, Napoli 80124, Italy

Abstract—This work deals with the inverse source problem starting from the knowledge of the radiated field in the near field zone. The inverse problem is stated as the inversion of a linear integral equation and the Singular Value Decomposition (SVD) is exploited as an analysis and inversion tool. In particular, here, we deal with a 2D geometry and aim at comparing the features of the inverse problem in dependence on the nature of the source (electric or magnetic).

1. INTRODUCTION

This work deals with the classical problem of the determination of a source current from the knowledge of the radiated field [1–4].

In particular, here, we consider the 2D geometry and a radiating source current supported over a bounded rectilinear domain while the radiated field is collected over a bounded rectilinear domain parallel to the source domain and located in the near zone.

Such a kind of analysis has been already performed for a magnetic rectilinear source, as shown in [5]. In general, this kind of problem is stated as a linear inverse one [6] and in order to investigate the performance of the inversion approach, the main effort is concerned with the determination of the Number of Degrees of Freedom (NDF) of the field in dependence of the geometrical properties (extent and distance) of the source and the observation domains. In this framework, a good analysis tool is represented by the Singular Value Decomposition (SVD) of the relevant operator [1, 6].

Received 5 July 2011, Accepted 3 August 2011, Scheduled 29 August 2011

* Corresponding author: Francesco Soldovieri (soldovieri.f@irea.cnr.it).

Aim of this paper is to investigate the different features of the two inverse source problems for the case of the magnetic and electric sources. In particular, the analysis is performed by the Singular Value Decomposition and the reconstruction performances are evaluated in terms of singular values behavior and regularized reconstruction of a pulse source via the truncated SVD.

Therefore, the paper is organized as follows.

Section 2 briefly sketches the formulation of the inverse source problem for both cases of the electric and magnetic source. Section 3 deals with the Singular Value Decomposition as a tool for the analysis and inversion of a linear compact operator. Section 4 is devoted to present the analysis of the two radiation operators and a comparison between the singular values behaviors is pointed out and investigated. Section 5 tackles the problem of the reconstruction of both magnetic and electric impulsive source starting from the knowledge of the field. Finally, conclusions follow.

2. FORMULATION OF THE INVERSE SOURCE PROBLEM FOR THE MAGNETIC AND ELECTRIC SOURCE

This section is devoted at presenting the mathematical formulation of the inverse source problem in the 2D geometry for both kinds of electric and magnetic source.

In particular, a rectilinear source is considered along the x-axis and with extent given by $S = [-X_S, X_S]$. The measurement domain, within which the radiated field is measured, is also assumed to be parallel to the x-axis, in near field at constant distance z_1 and with extent $O_1 = [-X_1, X_1]$ (see Figure 1 for the geometry of the problem).

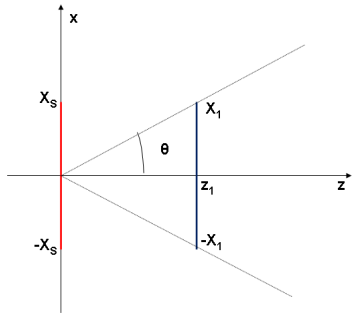

Figure 1. Geometry of the problem.

Now, for sake of simplicity, two separate subsections for magnetic and electric sources are presented, respectively. In particular, each subsection deals with the formulation of the related problem and the relevant radiation operator is sketched out.

In particular, we have considered the case of the magnetic source, because, also if the magnetic sources are not physical quantities, in many cases the radiation problems are given in terms of "equivalent" magnetic sources, as f.i. occurs for the aperture antennas.

2.1. Magnetic Source

This subsection deals with a magnetic source J_m, directed along the x-axis. In this case, the tangential component of the radiated field is directed along the y-axis and is given by

$$E(x, z_1) = \frac{\beta}{4j} \int_{-X_S}^{X_S} \frac{H_1^{(2)}(\beta r) z_1}{r} J_m(x') dx' \quad x \in O_1 \tag{1}$$

where $H_1^{(2)}(\cdot)$ is the Hankel function of second kind and first order, $\beta = \omega\sqrt{\varepsilon_0 \mu_0}$ is the wave-number of the free-space, being ε_0 and μ_0 the dielectric permittivity and the magnetic permeability of the free space, respectively, $r = \sqrt{(x - x')^2 + z_1^2}$ denotes the distance between the generic point of the source domain and the point of the measurement domain.

Relation (1) can be seen as a linear transformations

$$A : J_m \in L^2(S) \rightarrow E \in L^2(O_1) \tag{2}$$

Equation (2) means that the only a priori information about the magnetic current is that it is a square integrable function defined on the source domain S whereas the radiated field is assumed as a square integrable function defined on the measurement domain O_1.

2.2. Electric Source

We assume that the electric source J is directed along the y-axis. In this case, the tangential component of the radiated field is again directed along the y-axis and is given by [7]

$$E(x, z_1) = \frac{\omega \mu_0}{4j} \int_{-X_S}^{X_S} H_0^{(2)}(\beta r) J(x') dx' \quad x \in O_1 \tag{3}$$

where $H_0^{(2)}(\cdot)$ is the Hankel function of second kind and zero-th order.

Equation (3) can be interpreted as a linear transformation

$$B : J \in L^2(S) \rightarrow E \in L^2(O_1) \tag{4}$$

that relates the square integrable function electric current $J(x')$ defined on the source domain S to the radiated electric field over the measurement domain O_1.

3. THE INVERSE SOURCE PROBLEM

Accordingly to the outcomes of the previous Section, the problem of the reconstruction of the magnetic current J_m (or alternatively of the electric current J), starting from the knowledge of the radiated field over the observation domain O_1, can be stated as the inversion of the operator A (or of the operator B).

The operators A and B exhibit some common properties, but also few differences arise between them; here, we exploit SVD tool [6] in order to present the common and different features of the two operators.

As first common feature, the two radiation operators A and B are compact operators [1] and accordingly, it is possible to express them by exploiting the SVD. Here, the details for the SVD of the operator A are given; of course, the same considerations hold even for the operator B.

For the operator A, the singular system $\{\sigma_{An}, u_{An}, v_{An}\}_{n=0}^{\infty}$ can be defined [6], wherein: the series $\{\sigma_{An}\}_{n=0}^{\infty}$ denotes the singular values ordered in a non-increasing sequence; the set $\{u_{An}\}_{n=0}^{\infty}$ is the orthonormal basis for the subspace of the visible objects (i.e., the objects that could be retrieved by the error-free data); the set $\{v_{An}\}_{n=0}^{\infty}$ is the orthonormal basis for the closure of the range of the operator A.

A formal solution of the inverse problem is expressed as:

$$J_m(x') = \sum_{n=0}^{\infty} \frac{1}{\sigma_{An}} \langle E, v_{An} \rangle u_{An} \tag{5}$$

where $\langle \cdot, \cdot \rangle$ denotes the scalar product in the data space $L^2(O_1)$.

As a common feature of the two operators, for their compactness [1, 6], the relative singular values cluster to zero asymptotically (i.e., as their index tends to infinity); this entails that the related inversion problem at hand is ill-posed. Accordingly, in order to obtain a stable inversion of the operators in (1) and (3), the singular spectrum should be suitably truncated by accounting for the noise level on data [6, 8]. For the case at hand, it will be seen that the singular values of A and B exhibit an almost step-like behavior [1, 5]; this means that the singular values exhibit a limited dynamics (they are constant or almost constant) before a knee after that they decay exponentially fast.

Consequently, the inversion of A (and B) is a severely ill-posed problem [6]; this entails that the number of singular values to be retained in a regularized reconstruction scheme is essentially finite and, apart very low signal to noise ratio, is generally weakly dependent on noise level and regularization scheme. Accordingly, it is possible to identify the Number of Degrees of Freedom (NDF) of the radiated field just as the number of singular values before the asymptotic fast decay.

In this case, it is possible to adopt the Truncated SVD (TSVD) as regularization scheme; this scheme consists in truncating the series in (5) at an index N_T, so that the regularized solution is achieved by

$$\tilde{J}_m(x') = \sum_{n=0}^{N_T} \frac{1}{\sigma_{An}} \langle E, v_{An} \rangle u_{An} \tag{6}$$

where the index N_T acts as a regularization parameter.

All considerations above hold also for the case of the electric source and the relative operator B whose singular system is denoted by $\{\sigma_{Bn}, u_{Bn}, v_{Bn}\}_{n=0}^{\infty}$.

4. A COMPARISON BETWEEN THE SINGULAR VALUES FOR THE TWO OPERATORS

This section is devoted at analyzing the different behavior of the two sequences of the singular values for the two radiation operators.

First, the results relative to the case of the magnetic source are recalled [1, 5]. In particular, it is already found that the singular values behavior of the operator A is step-like; in fact, the singular values are constant before at a knee after which an exponential decay arises.

The knee arises at the singular value index

$$\tilde{N} \cong \left[\frac{2}{\lambda} (R_1 - R_2) \right] \tag{7}$$

where $R_1 = \sqrt{(X_S + X_1)^2 + z_1^2}$, $R_2 = \sqrt{(X_S - X_1)^2 + z_1^2}$ and λ is the wavelength.

Such a step-like behavior of the singular values permits to assume the number of degrees of freedom of the radiated field equal to the index $\tilde{N}$ given in (7), i.e., a severely ill-posed inverse problem has to be tackled [6] and the TSVD can be arrested at an index $N_T = \tilde{N}$.

Let us turn to present a comparison between the singular values of the two operators A and B. In particular, the comparison is performed between the two operators by neglecting the constant quantities outside

the integrals in (1) and (3), respectively. Accordingly, the two normalized operators are denoted by $\tilde{A}$ and $\tilde{B}$, respectively.

Now few mathematical considerations are in order. By assuming that $\beta r \gg 1$ (this entails that the observation domain is only at few wavelengths from the source domain) and by resorting to the asymptotic form of the Hankel functions for large argument, the relationship $H_n^{(2)}(\beta r) \approx \sqrt{\frac{2j}{\pi\beta r}} j^n e^{-j\beta r}$ holds [7].

Let us turn now to consider the operators given by (1) and (3); as a general rule, the following relation hold for the two operators

$$\int_{-X_1}^{X_1} dx \int_{-X_S}^{X_S} \left| \frac{H_1^{(2)}(\beta r) z_1}{r} \right|^2 dx' = \sum_{n=0}^{\infty} \tilde{\sigma}_{An}^2 \tag{8}$$

and

$$\int_{-X_1}^{X_1} dx \int_{-X_S}^{X_S} \left| H_0^{(2)}(\beta r) \right|^2 dx' = \sum_{n=0}^{\infty} \tilde{\sigma}_{Bn}^2 \tag{9}$$

By exploiting relations (8) and (9), it can be written

$$\begin{aligned} \sum_{n=0}^{\infty} \tilde{\sigma}_{An}^2 &= \int_{-X_1}^{X_1} dx \int_{-X_S}^{X_S} \left| \sqrt{\frac{2j}{\pi\beta r}} j e^{-j\beta r} \right|^2 \left| \frac{z_1}{r} \right|^2 dx' \\ &< \int_{-X_1}^{X_1} dx \int_{-X_S}^{X_S} \left| \sqrt{\frac{2j}{\pi\beta r}} e^{-j\beta r} \right|^2 dx' = \sum_{n=0}^{\infty} \tilde{\sigma}_{Bn}^2 \end{aligned} \tag{10}$$

and relation (10) makes possible to state that the summation of the square singular values of the normalized operator $\tilde{B}$ (electric source) is larger than the corresponding quantity for the operator $\tilde{A}$ (magnetic source). Anyway, it is worth noting that this statement does not permit us to state that for each index the singular value of the operator $\tilde{B}$ is larger than the homologous one of the operator $\tilde{A}$.

The theoretical statement in (10) is numerically confirmed by considering a source domain with semi-extent $X_s = 10\lambda$ and an observation domain at distance $z_1 = 5\lambda$ with varying semi-extent ranging in the interval $X_1 \in [\lambda, 20\lambda]$ with a step of λ. Red dashed

line of Figure 2 depicts the quantity

$$\text{Ratio} = \frac{\int_{-X_1}^{X_1} dx \int_{-X_S}^{X_S} \left| H_0^{(2)}(\beta r) \right|^2 dx'}{\int_{-X_1}^{X_1} dx \int_{-X_S}^{X_S} \left| \frac{H_1^{(2)}(\beta r) z_1}{r} \right|^2 dx'} \tag{11}$$

for the different values of the semi-extent of the observation domain ranging from λ to 20λ.

The same analysis has been performed also for the values of the distance z_1 ranging from 10λ to 25λ with a step of 5λ and the results in term of the ratio R are depicted in Figure 2. It can be observed that as long as the extent of the observation domain increases and/or the distance of the observation domain decreases, the term z_1/r has an increasing role in making different the two integrand functions involved in the numerator and the denominator of (11) and consequently to have a ratio R more and more different from one. Therefore, for a fixed value of the distance z_1, the two singular values behavior become more and more different as long as the extent of the observation domain increases.

This is pointed out from the figures below that are all concerned with the source semi-extent equal to $X_s = 10\lambda$ and a quota $z_1 = 5\lambda$.

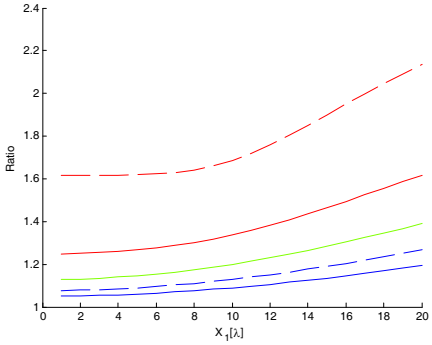

Figure 2. Ratio in Equation (11) depicted for different semi-extent of the observation domain: red dashed curve $z_1 = 5\lambda$; red dotted line $z_1 = 10\lambda$; green curve $z_1 = 15\lambda$; blue dashed line $z_1 = 20\lambda$; blue dotted line $z_1 = 25\lambda$.

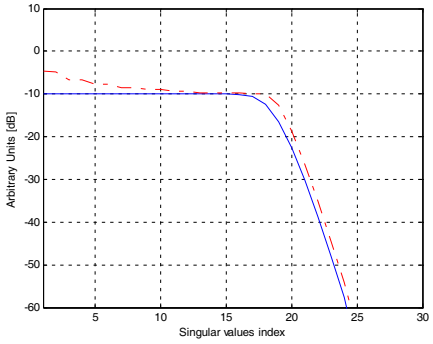

Figure 3. Comparison between the absolute singular values of the two normalized operators (blue line: magnetic source; red dashed line: electric source) in the case $X_1 = 5\lambda$ and $z_1 = 5\lambda$.

Table 1.

	$X_1 = 5\lambda$	$X_1 = 10\lambda$	$X_1 = 15\lambda$	$X_1 = 20\lambda$
$\tilde{N}$ estimated by (7)	17	31	37	38
Ratio between the first singular values of the two operators	1.82	2.22	2.60	2.97
Ratio R in (11)	1.62	1.68	1.90	2.14

Figure 3 depicts the case of a semi-extent of the observation domain equal to $X_1 = 5\lambda$. For this and the following figures, the red dashed line and blue solid line refer to the singular values of the electric and magnetic sources, respectively. The examination of this figure shows that the magnetic singular values exhibits a knee which arises at the index $\tilde{N} = 17$ as estimated by (7). The same step-like behavior also arises for the electric source whereas the dissimilarity between the two behaviors arises in the zone before the common exponential decay. In particular, it can be observed that the singular values for the electric source are larger than the corresponding ones of the magnetic source. Table 1 reports the ratio between the first (largest) singular values of the two operators and the quantity R defined in (11).

The same analysis has been performed for the further three cases of $X_1 = 10\lambda$, $X_1 = 15\lambda$ and $X_1 = 20\lambda$. Figures 4–6 depict the singular values behavior for these three cases and Table 1 reports the relative results. From the examination of the above figures and Table 1, some considerations follow.

First of all, the expected step-like behavior of the magnetic source (goodness of the estimate of the knee-index in (7)) is verified for all the presented cases and a similar step-like behavior even holds for the electric source.

Secondly, we verify that at the increase of the extent of the observation domain, the increasing role in the integral provided by the term z_1/r makes it possible a more evident difference between the singular values behaviors; this fact is also inferred by the values in the Table 1.

In addition, it has been numerically verified (and not shown here for sake of brevity) that, as expected, the same singular values behaviors even holds in the case that the role of the observation domain and the extent domain are interchanged. In other words, the figures above shown can continue to hold for the "reciprocal" case of

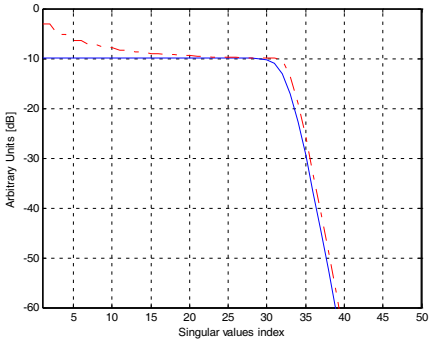

Figure 4. Comparison between the absolute singular values of the two operators (blue line: magnetic source; red dashed line: electric source) in the case $X_1 = 10\lambda$ and $z_1 = 5\lambda$.

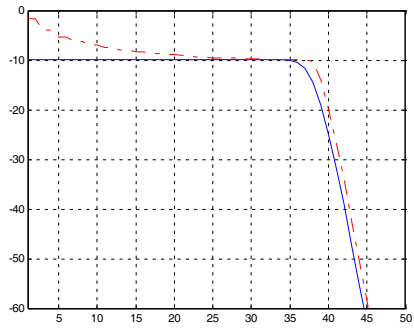

Figure 5. Comparison between the absolute singular values of the two operators (blue line: magnetic source; red dashed line: electric source) in the case $X_1 = 15\lambda$ and $z_1 = 5\lambda$.

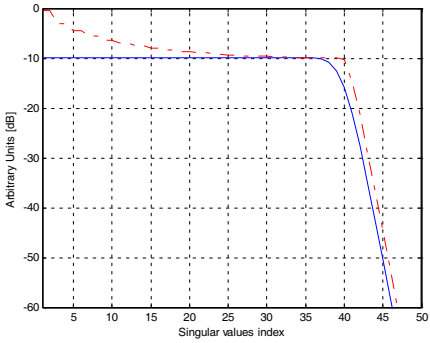

Figure 6. Comparison between the absolute singular values of the two operators (blue line: magnetic source; red dashed line: electric source) in the case $X_1 = 20\lambda$ and $z_1 = 5\lambda$.

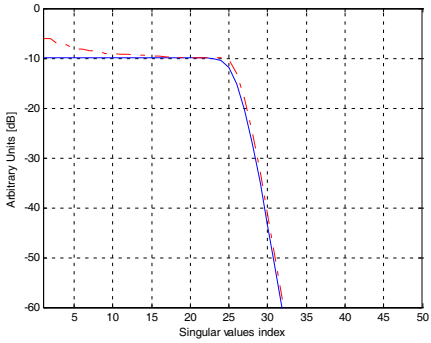

Figure 7. Comparison between the absolute singular values of the two operators (blue line: magnetic source; red dashed line: electric source) in the case $X_1 = 10\lambda$ and $z_1 = 10\lambda$.

the distance $z_1 = 5\lambda$ and the semi-extent of the observation domain $X_1 = 10\lambda$, while it is the semi-extent X_s of the source domain that ranges from 5λ to 20λ.

A further analysis has regarded also the case of the increase in the quota z_1 for an observation domain with fixed semi-extent $X_1 = 10\lambda$ (the semi-extent of the source is the same of the above case). In

particular, besides the quota $z_1 = 5\lambda$, already considered in Figure 4, other three quotas $z_1 = 10\lambda$, $z_1 = 15\lambda$ and $z_1 = 20\lambda$ are considered.

Figures 7–9 depict the comparison between the singular values in the cases of distance $z_1 = 10\lambda$, $z_1 = 15\lambda$ and $z_1 = 20\lambda$, respectively. Table 2 is the analogous of Table 1 where the varying parameter is the distance z_1. From the examination of Figures 7–9 and Table 2, it can be inferred that as long as the distance z_1 increases, the role of the factor z_1/r is less relevant in order to have a difference between the two kernels in (11), and the two singular values behaviors become more and more similar.

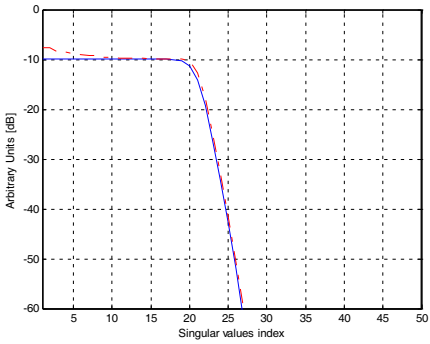

Figure 8. Comparison between the absolute singular values of the two operators (blue line: magnetic source; red dashed line: electric source) in the case $X_1 = 10\lambda$ and $z_1 = 15\lambda$.

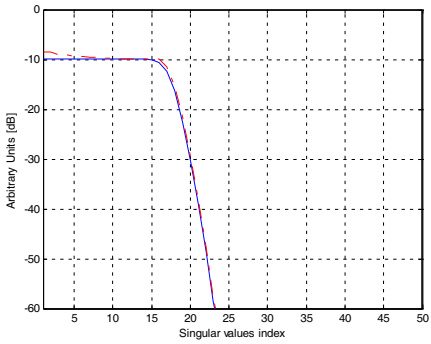

Figure 9. Comparison between the absolute singular values of the two operators (blue line: magnetic source; red dashed line: electric source) in the case $X_1 = 10\lambda$ and $z_1 = 20\lambda$.

Table 2.

	$z_1 = 5\lambda$	$z_1 = 10\lambda$	$z_1 = 15\lambda$	$z_1 = 20\lambda$
$\tilde{N}$estimated by (7)	31	25	20	16
Ratio between the first singular values of the two operators	2.22	1.56	1.30	1.18
Ratio in (11)	1.68	1.34	1.20	1.13

5. TRUNCATED SVD REGULARIZED POINT SPREAD FUNCTION

This section aims at presenting the features of the regularized reconstruction of a Dirac function, for the two normalised radiation operators $\tilde{A}$ and $\tilde{B}$, at variance of the TSVD threshold in (6). In such an analysis, the regularization parameter will be considered as the ratio between the minimum singular value retained in the TSVD summation and the maximum one.

The analysis is performed for the case of a source with semi-extent equal $X_s = 10\lambda$ and an observation domain at distance $z_1 = 5\lambda$ and with semi-extent $X_1 = 20\lambda$ (Figure 6 depicts the singular values behavior of the two operators). This case is chosen because the singular values of the two radiation operators exhibit a significant difference so that different performances are expected in the TSVD regularized reconstruction of the impulsive source.

This is shown in Figures 10–13 that depict the reconstruction of a unit-pulse function located at the center ($x = 0$) of the source domain. The examination of these figures allows to point out that when the TSVD threshold is high (the cases of TSVD threshold equal to 0.7 and 0.5) a significant difference in the reconstruction arises (see Figures 10, 11); this is due to the very different number of terms retained in TSVD expansion, as reported in Table 3.

Figures 10 and 11 permit us to state that the reconstruction with the magnetic source is reliable even with very low signal to noise ratio; differently, for the electric source, due to the decay of the singular values before the knee, the reconstruction results are completely unreliable since they do not permit to localize the pulse source.

Table 3.

TSVD Threshold	*Number of TSVD retained terms for the electric source*	*Number of TSVD retained terms for the magnetic source*
0.7	4	39
0.5	10	40
0.1	41	42
0.01	44	44

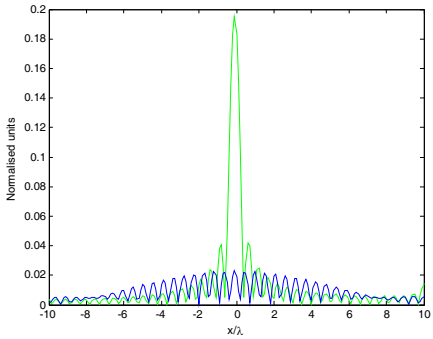

Figure 10. Comparison between the TSVD reconstruction of the pulse function located at $x = 0$. (green line: magnetic source; blue line: electric source). TSVD threshold equal to 0.7.

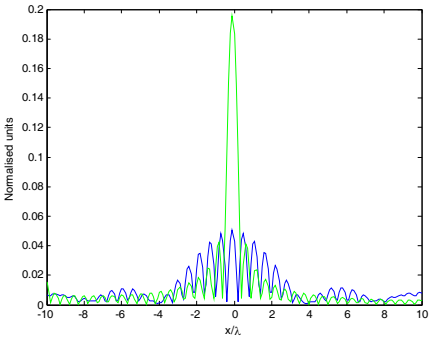

Figure 11. Comparison between the TSVD reconstruction of the pulse function located at $x = 0$. (green line: magnetic source; blue line: electric source). TSVD threshold equal to 0.5.

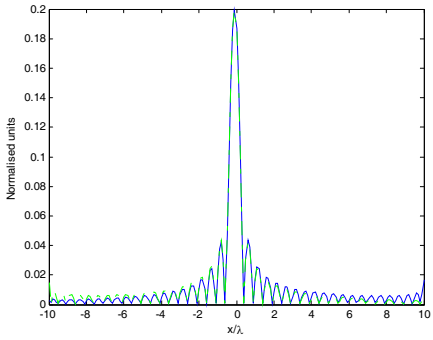

Figure 12. Comparison between the TSVD reconstruction of the pulse function located at $x = 0$. (green line: magnetic source; blee line: electric source). TSVD threshold equal to 0.1.

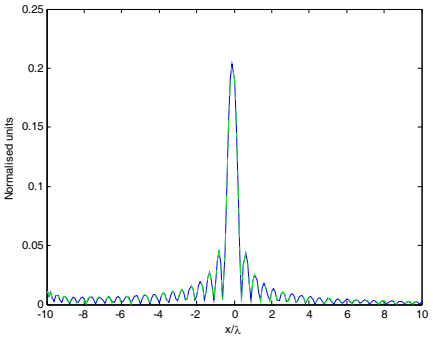

Figure 13. Comparison between the TSVD reconstruction of the pulse function located at $x = 0$. (green line: magnetic source; blue line: electric source). TSVD threshold equal to 0.01.

Conversely, the reconstructions become quite similar in the other two cases (TSVD threshold equal to 0.1, 0.01) where the TSVD expansion involves almost the same number of terms (see Table 3).

These reconstruction results permit also to point out how the subspace spanned by the singular functions in the unknown space becomes very similar when all the singular values before the common exponential decay are considered.

A comparison between the reconstruction performance of the inversion approach in the two cases can be also shown by pointing out the different spectral contents defined as

$$SP(u) = \sum_{n=0}^{N_T} \left| \widehat{u}_n(u) \right| \tag{12}$$

where

$$\widehat{u}_n(u) = \int_{-X_S}^{X_S} u_n(x) \exp(-jux) dx \tag{13}$$

represents the Fourier transform of the n-th right singular function $u_n(x)$.

The spectral content accounts for the class of the retrievable harmonic content on dependence of the measurement configuration and the choice of the TSVD regularization parameter [9–11]. Figures 14 and 15 depict the spectral content for the cases of the magnetic and electric source, respectively, and for different values of the TSVD threshold (the above mentioned ones and the additional TSVD threshold equal to 0.3). A different behavior can be observed; for the magnetic source the same spectral content arises for the different TSVD threshold (Figure 14). The situation changes in the case of the electric (see Figure 15) source where for the cases of TSVD threshold equal to 0.7 and 0.5, a strong filtering effect for the low spatial frequencies (low values of u) can be observed, which disappears as the TSVD threshold becomes smaller.

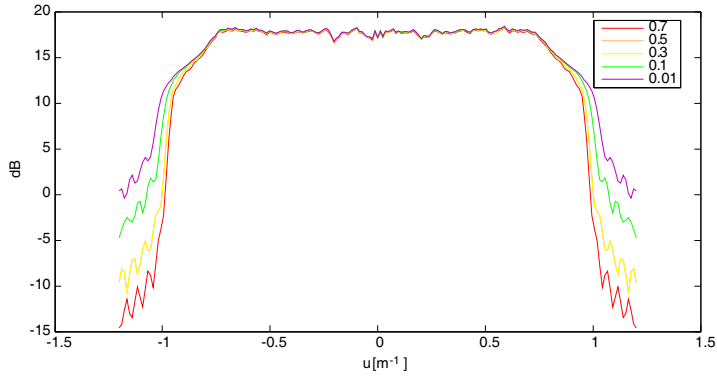

Figure 14. Spectral content for the magnetic source and different TSVD thresholds.

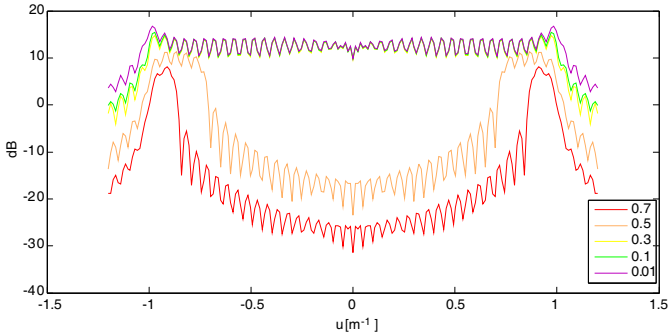

Figure 15. Spectral content for the electric source and different TSVD thresholds.

6. CONCLUSIONS

In this work, a comparison between the two radiation operators concerned with the electric source and magnetic source is presented. The analysis has been performed by means of the SVD tool that have permitted to discuss the reconstruction performances of the two formulations.

In particular, the analysis has shown that for the electric source, the singular values are larger compared to the ones of the magnetic source but at the same time they exhibit a smooth variation before the exponential decay, which occurs an index that is, approximately the same for a magnetic source.

Consequently, for low values of the signal to noise ratio, the quality of the reconstruction of an electric source is significantly dependent on the threshold fixed for TSVD and on the distance from source and observation domain.

REFERENCES

1. Pierri, R. and F. Soldovieri, "On the information content of the radiated fields in the near zone over bounded domains," *Inverse Problems*, Vol. 14, No. 2, 321–337, Apr. 1998.
2. Solimene, R. and R. Pierri, "Number of degrees of freedom of the radiated field over multiple bounded domains," *Opt. Lett.*, Vol. 32, 3113–3115, 2007.
3. Bucci, O. M., C. Gennarelli, G. Riccio, and C. Savarese, "Sampling representation of electromagnetic fields over three-dimensional domains," *Radio Science*, Vol. 34, 567–574, 1999.

4. Sten, J. C.-E. and E. A. Marengo, "Inverse source problem in an oblate spheroidal geometry," *IEEE Transactions on Antennas and Propagation*, Vol. 54, 3418–3428, 2006.
5. Soldovieri, F., C. Mola, R. Solimene, and R. Pierri, "Inverse source problem from the knowledge of radiated field over multiple rectilinear domains," *Progress In Electromagnetics Research M*, Vol. 8, 131–141, 2009
6. Bertero, M. and P. Boccacci, *Introduction to Inverse Problems in Imaging*, Institute of Physics, Bristol, UK, 1998.
7. Balanis, C. A., *Advanced Engineering Electromagnetics*, John Wiley & Sons, Publishers, Inc., New York, 1989.
8. Bertero, M., C. de Mol, and G. A. Viano, "The stability of inverse problems, in inverse scattering problems," *Optics*, H. P. Baltes (ed.), Topics in Current Physics, Vol. 20, 161–214, Springer, Berlin, 1980.
9. Leone, G. and F. Soldovieri, "Analysis of the distorted Born approximation for subsurface reconstruction: Truncation and uncertainties effect," *IEEE Trans. Geoscience and Remote Sensing*, Vol. 41, No. 1, 66–74, Jan. 2003.
10. Persico, R., G. Alberti, G. Esposito, G. Leone, and F. Soldovieri, "On multifrequency strategies of use of G.P.R. systems," *Proc. of SPIE*, Vol. 4123, Image Reconstruction from Incomplete Data, San Diego, USA, Aug. 2000.
11. Persico, R., "On the role of measurement configuration in contactless GPR data processing by means of linear inverse scattering," *IEEE Trans. Ant. Prop.*, Vol. 54, No. 7, 2062–2071, Jun. 2006.